Momentum and Thermal Slip Conditions of an MHD Double Diffusive Free Convective Boundary Layer Flow of a Nanofluid with Radiation and Heat Source/Sink Effects

*Eshetu Haile Gorfie[1], Bandari Shankar[2]
[*1]Osmania University, Department of Mathematics, Hyderabad 500 007, eshetuhg@gmail.com
[2]Osmania University, Department of Math., Hyderabad 500 007, bandarishanker@yahoo.com

Abstract

In this paper, momentum and thermal slip conditions of an MHD double diffusive free convective boundary layer flow of a nanofluid with radiation and heat source/sink effects past a vertical semi-infinite flat plate are presented. The sheet is situated in a free stream in the xz-plane and y is measured normal to the surface directing to the positive y-axis. A variable transverse magnetic field is applied parallel to the y-axis. Effects of magnetic field, heat source/sink and thermal radiation have been studied on the flow quantities in addition to others' effects as mentioned in the literature. The governing boundary layer equations of the problem are formulated and then transformed into dimensionless equations. The resulting equations are solved numerically by the fourth order Runge-Kutta integration scheme in conjunction with the shooting method. Finally, effects of the pertinent parameters on velocity, temperature, solute concentration, nanoparticle volume fraction, skin friction coefficient, Nusselt number, regular mass transfer rate and nanoparticle mass transfer rate are briefly mentioned and justified graphically and in tabular form. The results are in nice agreement with that of the papers under considerations as mentioned in the literature.

Keywords: Momentum Slip; Thermal Slip; Brownian Diffusion; Thermophoresis; Thermal Radiation; Magnetic Field; Heat Source/Sink; Vertical Flow

1. Introduction

Nanofluids are dilute liquid suspensions of nanoparticles with dimensions smaller than100 nm. Nanofluids have been found to possess enhanced thermophysical properties compared to base fluids like oil or water [1]. Thermo-physical properties of nanofluids depend on nanoparticle volumetric fraction, aggregation of nanoparticle, size and shape of the nanomaterials [2]. Nanofluids possess wide range applications in science and technology [3]. The pioneering work on enhancing thermal conductivity of fluids with nanoparticles was studied by Choi [4]. Abnormal increase of thermal conductivity and viscosity of nanofluids with respect to base fluids was examined by Buongiorno [5].

Crane [6] did the pioneering work of his study on boundary layer flow over a stretching surface. This area is becoming novel area of research owing to its engineering applications in metallurgy and polymer technologies as the final product of the desired characteristics depend on the rate of cooling and in the process of stretching. The analytical model suggested by Buongiorno [5] for convective transport of nanofluids includes Brownian motion and thermophoresis. Many authors have been used this model. Khan and Aziz [7] used the model in their study of natural convection flow of a nanofluid over a vertical plate with uniform surface heat flux. On the other hand, Kuznetsov and Nield [8] extended the classical problem of free convection of an ordinary fluid along an isothermal vertical plate to the flow of a nanofluid. The gap between the works of [7] and [8] have been filled by Aziz and Khan [9] by using a comprehensive thermal convective boundary condition to study free convective nanofluids flows. Furthermore, studies on free and forced convective boundary layer flows of nanofluids in a vertical motion at different conditions have been conducted by many researchers [10-16]. Due to the wide range applications in

chemical engineering, solid state physics, oceanography, geophysics, etc, researches on double diffusive phenomena are becoming popular and are attracting the attentions of many researchers. Nield and Kuznetsov [14] examined double diffusive natural convective boundary layer flow in a porous medium saturated by a nanofluid. The authors used Buongiorno's model for nanofluid and Darcy's model for the porous medium term. Moreover, Khan and Aziz [17] studied on double diffusive natural convective boundary layer flow in a porous medium saturated with a nanofluid over a vertical plate. MHD flow past a flat surface has many important technological and industrial applications such as micro MHD pumps, micromixing of physiological samples, biological transportation and drug delivery [18–19]. Yazdi [20] further elaborated the application of a magnetic field that it produces Lorentz forces which are able to transport liquids in the mixing processes as an active micromixing technology method. In addition to this, Uddin et al.[21] pointed out that a magnetic nanofluid has many applications: magnetofluidic

Nomenclature

a	Momentum slip parameter	Pr	Prandtl number
b	Thermal slip parameter	Q	Heat source/sink parameter
B	Magnetic field strength	Ra_x	Local Rayleigh number
C	Solutal concentration	R	Radiation parameter
C_f	Skin friction coefficient	Sh_x	Regular Sherwood number
C_w	Solutal concentration at the vertical plate	Sh_{xn}	Nanoparticle Sherwood number
C_∞	Ambient solutal concentration	T	Fluid temperature
D_1	Thermal slip factor	T_w	Temperature at the vertical surface
D_B	Brownian motion diffusion coefficient	T_∞	Ambient temperature
D_T	Thermophoretic diffusion coefficient	u, v	Velocity components in the x-and y- axes
D_{CT}	Soret type diffusivity	$x; y$	Cartesian coordinates measured along and normal to the stretching sheet
D_{TC}	Dufour type diffusivity		
D_S	Solutal diffusivity		

Greek Symbols

f	Dimensionless stream function	α	Thermal diffusivity of the base fluid
g	Dimensionless solutal concentration	β_C	Coefficient of solutal expansion
g^*	Acceleration due to gravity	β_T	Coefficient of thermal expansion
h	Dimensionless nanoparticle fraction	θ	Dimensionless temperature
k	Thermal conductivity of the nanofluid	σ	Electrical conductivity of the fluid
k^*	Rosseland mean absorption coefficient	σ^*	Stefan-Boltzmann constant
k_f	Thermal conductivity of the base fluid	ψ	Stream function
Ld	Dufour solutal Lewis number	$\emptyset$	Nanoparticles volume fraction
Le	Regular Lewis number	η	Dimensionless similarity variable
Ln	Nanofluid Lewis number	γ	Dimensionless heat source/sink parameter
M	Magnetic parameter	μ	Dynamic viscosity of the nanofluid
N_1	Momentum slip factor	υ	Kinematic viscosity of the fluid
Nb	Brownian motion parameter	ρ_f	Density of the base fluid
Nc	Regular buoyancy ratio	ρ_p	Density of the nanoparticle
Nd	Modified Dufour parameter	τ	A parameter defined by $\frac{(\rho C_p)_p}{(\rho C_p)_f}$
Nr	Nanofluid buoyancy parameter	$(\rho C_p)_f$	Heat capacity of the base fluid
Nt	Thermophoretic parameter	$(\rho C_p)_p$	Heat capacity of the nanoparticle
Nu_x	Nusselt number		

leakage-free rotating seals, magnetogravimetric separations, acceleration/inclinations sensors, aerodynamic sensors (differential pressure, volumic flow), nano/micro-structured magnetorheological fluids for semi active vibration

dampers, biomedical applications in plant genetics and veterinary medicine. Later, Chamkha and Aly [22] studied MHD free convection flow of a nanofluid past a vertical plate in the presence of heat generation or absorption effects. Recently, the influence of thermal and solutal stratification parameters on natural convection boundary layer flow of a nanofluid past a vertical plate embedded in a porous medium has been briefly stated by Srinivasacharya and Surender [23]. The authors followed non-similar solution procedures as their methodology. On the other hand, Olanrewaju et al.[24] investigated double diffusive convection from a permeable vertical surface under convective boundary condition in the presence of heat generation and thermal radiation.

The above studies were engaged in the conventional no slip boundary conditions at the plate surface. The no slip boundary condition, which is the assumption that a liquid sticks to a solid boundary, is one of the pillars of the Navier–Stokes theory. However, there are situations where this condition fails. Partial velocity slip may occur on the stretching boundary when the fluid is particulate such as emulsions, suspensions, foams and polymer solutions [25]. The non-adherence of the fluid to a solid boundary is called velocity slip. Moreover, B´eg et al.[26] explained that the no slip conditions yield unrealistic behaviour and slip has to be incorporated to certain situations. These include the spreading of a liquid on solid substrates, corner flow and the extrusion of polymer melts from a capillary tube. No-slip conditions must be also replaced by slip conditions in microfluidics and nanofluidics. The concept of applying a convective boundary condition, which is the generalization of isothermal and thermal slip boundary condition, was introduced by Aziz [27]. Later, Nandeppanavar et al.[28] studied second order slip flow and heat transfer over a stretching sheet with non-linear Navier boundary condition. Momentum and thermal slip effects on double diffusive free convective boundary layer flow of a nanofluid was briefly explained by Khan et al.[29].Studies on MHD free convective boundary layer flow of nanofluids are very limited. As we have seen so far, effects of momentum and thermal slip conditions to double diffusive free convective boundary layer flows of nanofluids in a vertical flow have been dealt by many authors.

We didn't see a report incorporating effects of magnetic field, thermal radiation, heat source, etc. But such flows have to be studied because the contributions of these physical conditions may not be neglected in certain physical situations (as stated above in the third paragraph). The paper entitled "Momentum and thermal slip conditions of an MHD double diffusive free convective boundary layer flow of a nanofluid with radiation and heat source or sink effects" is considered; so far, the entitled manuscript has not been reported. We have extended the works of Khan et al.[29] by considering magnetic field, heat source/sink and thermal radiation effects to the flow regime for more physical implications. In addition to this, the roles of the other parameters are explained in brief. The results are displayed in figures and tables. For some pertinent parameters involving in the governing equations, physical interpretations to the results have been discussed. The governing equations are transformed to a couple of nonlinear ODEs using similarity transformations. The resulting equations are solved numerically by using a shooting method followed by the fourth order Runge-Kutta integration scheme. Effects of the pertinent parameters in the governing equations on velocity, temperature, solute concentration, nanoparticle volume fraction, skin friction coefficient, wall heat, regular mass and nanoparticle mass transfer rates are investigated.

2. Formulation of the Problem

A steady two-dimensional free convective boundary layer flow of a nanofluid moving along a semi- infinitely long vertical stationary flat plate in a moving free stream is considered as shown in Fig.1. The origin is located at the leading edge of the plate with the positive x-axis directing along the plate in the upward direction whereas y is measured normal to the plate and pointing in the positive y-axis. Let the plate be maintained at a uniform and constant solutal concentration C_w and nanoparticle volume fraction $\emptyset_w$. Let temperature of the wall be T_w, which is constant and let T_∞, C_∞ and $\emptyset_\infty$ be the ambient temperature, solute concentration and nanoparticle volume fraction, respectively. It is worth mentioning that $T_w > T_\infty$, $C_w > C_\infty$ and $\emptyset_w > \emptyset_\infty$ and as a result of this momentum, thermal, solutal and nanoparticle concentration boundary layers are formed near the solid surface. Hydrodynamic (momentum) and thermal slip conditions were considered at the solid interface. A variable transverse magnetic field $B(x)$ is applied to the flow along the y-axis. Heat source/sink and thermal radiation effects are considered. As the induced magnetic field is very small compared to the applied magnetic field, its effect is omitted. Considering these assumptions along with the model developed by Kuznetsov and Nield [30] with double diffusive condition, the governing equations for the flow in dimensional form can be written as:

$$\frac{\partial u}{\partial x} + \frac{\partial v}{\partial y} = 0 \tag{1}$$

$$\rho_f \left(u\frac{\partial u}{\partial x} + v\frac{\partial u}{\partial y} \right) = \mu \frac{\partial^2 u}{\partial y^2} + [(1-\phi_\infty)\rho_f g^*\{\beta_T(T-T_\infty)+\beta_C(C-C_\infty)\} - g^*(\rho_p - \rho_{f\infty})(\emptyset - \emptyset_\infty)]$$
$$-\sigma B^2 u, \tag{2}$$

$$u\frac{\partial T}{\partial x} + v\frac{\partial T}{\partial y} = \alpha\frac{\partial^2 T}{\partial y^2} + \tau\left[D_B\frac{\partial \emptyset}{\partial y}\frac{\partial T}{\partial y} + \frac{D_T}{T_\infty}\left(\frac{\partial T}{\partial y}\right)^2\right] + \frac{D_{TC}}{T_\infty}\frac{\partial^2 C}{\partial y^2} - \frac{1}{(\rho C_p)_f}\frac{\partial q_r}{\partial y} + \frac{Q}{(\rho C_p)_f}(T - T_\infty), \qquad (3)$$

$$u\frac{\partial C}{\partial x} + v\frac{\partial C}{\partial y} = D_S\frac{\partial^2 C}{\partial y^2} + \frac{D_{CT}}{T_\infty}\frac{\partial^2 T}{\partial y^2}, \qquad (4)$$

$$u\frac{\partial \emptyset}{\partial x} + v\frac{\partial \emptyset}{\partial y} = D_B\frac{\partial^2 \emptyset}{\partial y^2} + \frac{D_T}{T_\infty}\frac{\partial^2 T}{\partial y^2}, \qquad (5)$$
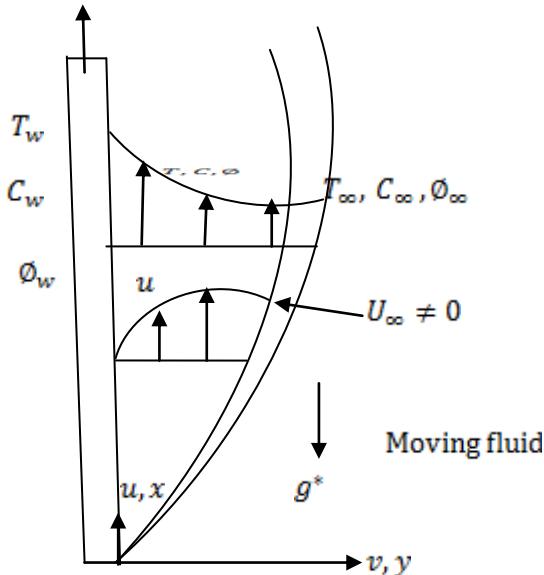
Fig. 1
Physical model and coordinate system

where $\alpha = \frac{k}{(\rho C_p)_f}$, q_r is the radiative heat flux, $B = B_0 x^{-1/4}$ for a constant $B_0 > 0$, $\tau = \frac{(\rho C_p)_p}{(\rho C_p)_f}$ and $Q = Q_0 x^{-1/2}$ for a constant Q_0. Here, μ, k, β_T, β_C are respectively viscosity, thermal conductivity, volumetric thermal expansion coefficient and volumetric solutal expansion coefficient of the nanofluid.

The corresponding boundary conditions to the governing equations are:

$$u = N_1 v\frac{\partial u}{\partial y}, \quad v = 0, \quad T = T_w + D_1\frac{\partial T}{\partial y}, \quad C = C_w, \quad \phi = \phi_w \text{ at } y = 0, \qquad (6)$$

$$u = c\sqrt{x}, \ T \to T_\infty, \ C \to C_\infty, \ \phi \to \phi_\infty \ \text{ as } y \to \infty,$$

where N_1 is hydrodynamic slip factor with dimension $(velocity)^{-1}$ and D_1 is thermal slip factor with dimension length. c is constant defined by $c = \alpha\sqrt{Ra}$ and $Ra = \frac{g\beta_T(1-\phi_\infty)(T_w-T_\infty)}{\alpha v}$.

The Rosseland diffusion approximation for radiation, q_r is defined by

$$q_r = -\frac{4\sigma^*}{3k^*}\frac{\partial T^4}{\partial y}. \qquad (7)$$

We assume that temperature differences within the flow are small so that T^4 can be expressed as a linear function of temperature and its Taylor series expansion about T_∞ neglecting higher order terms is $T^4 \cong 4TT_\infty^3 - 3T_\infty^4$ and $\frac{\partial q_r}{\partial y}$ becomes

$$\frac{\partial q_r}{\partial y} = -\frac{16\sigma^* T_\infty^3}{3k^*}\frac{\partial^2 T}{\partial y^2}. \qquad (8)$$

To transform the governing equations into a system of ODEs, the following non-dimensional quantities are introduced:

$$\eta = \frac{y}{x} Ra_x^{1/4}, \quad Ra_x = Rax^3, \quad \psi = \alpha Ra_x^{1/4} f(\eta), \quad T = T_\infty + (T_w - T_\infty)\theta(\eta),$$

$$C = C_\infty + (C_w - C_\infty)g(\eta), \quad \emptyset = \emptyset_\infty + (\emptyset_w - \emptyset_\infty)h(\eta). \tag{9}$$

Using the stream function ψ and the definitions

$u = \frac{\partial \psi}{\partial y}$ and $v = -\frac{\partial \psi}{\partial x}$, it can be easily shown that $u = \frac{\alpha}{x} Ra_x^{1/2} f'(\eta), v = \frac{\alpha}{x} Ra_x^{1/2}\left(\frac{\eta}{4}f'(\eta) - \frac{3}{4}f(\eta)\right)$

and the continuity equation (1) is identically satisfied. Substitution of the similarity variables into equations (2)-(5) give:

$$f''' + \frac{1}{4Pr}\left(3f f'' - 2f'^2\right) + \theta + Ncg - \text{Nr}h - Mf' = 0, \tag{10}$$

$$\left(1 + \frac{4}{3}R\right)\theta'' + \frac{3}{4}f\theta' + Nb\theta'h' + Nt\theta'^2 + Ndg'' + \gamma\theta = 0, \tag{11}$$

$$g'' + \frac{3}{4}Lefg' + Ld\theta'' = 0, \tag{12}$$

$$h'' + \frac{3}{4}Lnfh' + \frac{Nt}{Nb}\theta'' = 0, \tag{13}$$

and the corresponding boundary conditions become

$$f(0) = 0, \quad f'(0) = af''(0), \quad \theta(0) = 1 + b\theta'(0), \quad g(0) = 1, \quad h(0) = 1, \tag{14}$$

$$f'(\eta) \to 1, \quad \theta(\eta) \to 0, \quad g(\eta) \to 0, \quad h(\eta) \to 0, \quad \text{as } \eta \to \infty.$$

Here, primes denote differentiation with respect to η and the parameters are defined by $Pr = \frac{v}{\alpha}$ (Prandtl number), $Le = \frac{\alpha}{D_s}$ (Regular Lewis number), $Ln = \frac{\alpha}{D_B}$ (Nanofluid Lewis number), $Ld = \frac{D_{CT}}{D_s}\frac{(T_w - T_\infty)}{(C_w - C_\infty)}$ (Dufour solutal Lewis number), $R = \frac{4\sigma^* T_\infty^3}{kk^*}$ (Radiation parameter), $Nb = \frac{\tau D_B(C_w - C_\infty)}{\alpha}$ (Brownian motion parameter), $Nc = \frac{\beta_C}{\beta_T}\frac{(C_w - C_\infty)}{(T_w - T_\infty)}$ (Regular buoyancy ratio), $Nd = \frac{D_{TC}}{\alpha}\frac{(C_w - C_\infty)}{(T_w - T_\infty)}$ (Modified Dufour parameter), $Nr = \frac{(\rho_p - \rho_{f\infty})(\emptyset_w - \emptyset_\infty)}{\rho_{f\infty}\beta_T(1 - \phi_\infty)(T_w - T_\infty)}$ (Nanofluid buoyancy ratio parameter), $M = \frac{\sigma B_0^2}{\mu Ra^{1/2}}$ (Magnetic parameter), $Nt = \frac{\tau D_T}{\alpha T_\infty}\frac{(T_w - T_\infty)}{T_\infty}$ (Thermophoresis parameter), $\gamma = \frac{Q_0}{K Ra^{1/2}}$ (Heat source/sink parameter), $Ra_x = \frac{g\beta_T(1 - \phi_\infty)(T_w - T_\infty)}{\alpha v}x^3$ (Local Rayleigh number), $a = N_1 v Ra^{1/2}x^{-1/4}$ (Momentum slip parameter) and $b = D_1 Ra^{1/4}x^{-1/4}$ (Thermal slip parameter).

It is worth mentioning that for a quiescent free stream, $f'(\eta) \to 0$ as $\eta \to \infty$. If we consider the conventional no slip boundary conditions ($a = 0$), isothermal plate ($b = 0$) and excluding effects of magnetic field, radiation and heat source/sink from the flow field will reduce it to that of Kuznetsov and Nield [30]. On the other hand, the absence of magnetic field, thermal radiation and heat source/sink terms from this paper reduces it to that of Khan et al.[29].

The quantities with practical interest in the study are skin friction coefficient C_f, Nusselt number Nu_x, regular Sherwood number Sh_x and nanoparticle Sherwood number $Sh_{x,n}$. These parameters characterize surface drag, wall heat transfer, regular mass transfer and nanoparticle mass transfer rates, respectively.

These quantities are defined as:

$$C_f = \frac{2\tau_w}{\rho U_w^2}, \qquad Nu_x = \frac{xq_w}{k(T_w - T_\infty)}, \qquad Sh_x = \frac{xJ_w}{D_S(C_w - C_\infty)}, \qquad Sh_{x,n} = \frac{xJ_{np}}{D_B(\emptyset_w - \emptyset_\infty)} \tag{15}$$

where τ_w, q_w, J_w and J_{np} are the skin friction, wall heat flux, solutal wall mass flux and nanoparticle wall mass flux and they respectively, are defined according to Ram Reddy et al.[31] as

$$\tau_w = \mu\left(\frac{\partial u}{\partial y}\right)_{y=0}, \quad q_w = -\left(k + \frac{16\sigma^* T_\infty^3}{3k^*}\right)\left(\frac{\partial T}{\partial y}\right)_{y=0}, \quad J_w = -D_S\left(\frac{\partial C}{\partial y}\right)_{y=0}, \quad J_{np} = -D_B\left(\frac{\partial \emptyset}{\partial y}\right)_{y=0}. \quad (16)$$

Using the definitions of (16) and inserting them in (15), we get the dimensionless skin friction coefficient (surface drag), wall heat transfer, regular mass transfer and nanoparticle mass transfer rates respectively are

$$Ra_x^{1/4} C_f = 2Pr f''(0), \quad \frac{Nu_x}{Ra_x^{1/4}} = -\left(1 + \frac{4}{3}R\right)\theta'(0), \quad \frac{Sh_x}{Ra_x^{1/4}} = -g'(0) \text{ and } \quad \frac{Sh_x}{Ra_x^{1/4}} = -h'(0). \quad (17)$$

3. Numerical solution

As equations (10)-(13) are highly non-linear ODEs, it is difficult or impossible to find the closed form solutions. Thus, the equations with the boundary conditions (14) are solved numerically with the help of the shooting technique along with the fourth order Runge-Kutta integration scheme.

Our aim is to convert the boundary value problem in to an initial value problem as shown below: Let $f_1 = f$, $f_2 = f_1'$, $f_3 = f_2'$, $f_4 = \theta$, $f_5 = f_4'$, $f_6 = g$, $f_7 = f_6'$, $f_8 = h$ and $f_9 = f_8'$, then

$$f''' = -\frac{1}{4Pr}(3f_1 f_3 - 2f_2^2) - f_4 - Ncf_6 + Nrf_8 + Mf_2, \quad (18)$$

$$\theta'' = -\frac{1}{1+\frac{4}{3}R+NdLd}\left(\frac{3}{4}f_1 f_5 + Nbf_5 f_9 + Nt(f_5)^2 + \gamma f_4 - \frac{3}{4}NdLe f_1 f_7\right), \quad (19)$$

$$g'' = -\frac{3}{4}Le.f_1 f_7 + \frac{Ld}{1+\frac{4}{3}R+NdLd}\left(\frac{3}{4}f_1 f_5 + Nbf_5 f_9 + Nt(f_5)^2 + \gamma f_4 - \frac{3}{4}NdLe f_1 f_7\right) \text{ and } \quad (20)$$

$$h'' = -\frac{3}{4}Ln.f_1 f_9 + \frac{Nt}{Nb(1+\frac{4}{3}R+NdLd)}\left(\frac{3}{4}f_1 f_5 + Nbf_5 f_9 + Nt(f_5)^2 + \gamma f_4 - \frac{3}{4}NdLe f_1 f_7\right) \quad (21)$$

with the boundary conditions

$$f_1(0) = 0, \quad f_2(0) = af_3(0), \quad f_4(0) = 1 + bf_5(0), \quad f_6(0) = 1, f_8(0) = 1$$
$$f_2(\infty) = 1, \quad f_4(\infty) = 0, \quad f_6(\infty) = 0, f_8(\infty) = 0. \quad (22)$$

In order to integrate equations (18) - (21) and (22) as an initial value problem, we require values for $f_3(0) := p$, $f_5(0) := q$, $f_7(0) := r$ and $f_9(0) := d$ that is $f''(0)$, $\theta'(0)$, $g'(0)$ and $h'(0)$, respectively. Such values are not given in the boundary conditions (22). Thus, finding these values is our prime concern for various values of the given physical parameters.

The most important task of shooting method is to choose the appropriate finite values of η_∞. In order to determine η_∞ for the boundary value problem stated by equations (18)-(21), we start with some initial guess values for some particular set of physical parameters to obtain $f''(0)$, $\theta'(0)$, $g'(0)$ and $h'(0)$ differ by pre-assigned significant digit. The last value of η_∞ is finally chosen to be the most appropriate value of the limit η_∞ for that particular set of parameters. The value of η_∞ may change for another set of physical parameters. Once the finite value of η_∞ is determined, then the integration is carried out as stated by Mandal and Mukhopadhyay [32]. Accordingly, the initial condition vector for the boundary value problem is given by $[f(0), f'(0), f''(0), \theta(0), \theta'(0), g(0), g'(0), h(0), h'(0)]$ that is $Y_0 = [0, ap, p, 1 + bq, q, 1, r, 1, d]$.

We took the series of values for $f''(0)$, $\theta'(0)$, $g'(0)$ and $h'(0)$ and applied the fourth order Runge – Kutta integration scheme with step size $h = 0.01$. The above procedure was repeatedly performed till we obtained the desired degree of accuracy, 10^{-7}.

4. Results and Discussion

As it is briefly explained by Khan et al.[29], fluid velocity increases with increasing values of hydrodynamic slip parameter a where as it decreases with the increasing values of thermal slip parameter b for both mono and double-diffusive processes in the nanofluid. In addition to this, the authors investigated that the dimensionless temperature,

Table 1: Comparison of wall heat transfer rate for different values of Pr of the present study with earlier reports are shown below:

Pr	$-\theta'(0)$		
	Kuznetsov and Nield [30]	Khan et al.[29]	Present Study
0.71	0.387	0.3909	0.3868
1	0.401	0.4044	0.4010
2	0.426	0.4293	0.4260
10	0.465	0.4680	0.4649
100	0.490	0.4909	0.4873
1000	0.499	0.5010	0.4922

solute and nanoparticle concentrations decrease with increasing values of both the momentum and the thermal slip parameters. Our attention in this paper is not to mention what has been discussed so far rather we mainly focus on effects of the other parameters to the various physical quantities of the flow.

To investigate influences of the pertinent parameters on the flow quantities, a parametric study has been conducted. Effects of the various parameters like, magnetic M, heat source/sink γ, radiation R, Brownian motion Nb , thermophoresis Nt, regular buoyancy ratio Nc, modified Dufour Nd, nanofluid buoyancy ratio Nr, regular Lewis number Le, nanofluid Lewis number Ln, Dufour solutal Lewis number Ld and Prandtl number Pr; the numerical results are displayed graphically (Figs.2–Fig.28) and in tables (Table2 – Table 5). Accuracy of the method is validated by comparisons with the numerical results reported by Kuznetsov and Nield [30] and Khan et al.[29] for various Values of the reduced Nusselt number. For this, different values of Pr and $Le = Ld = 1,\ \gamma = 0,$ $R = M = 0 = a = b,\ Nb = Nt = Nr = Nc = Nd = 10^{-5}$ and $Ln = 10$ are considered. The comparison is as shown in table 1 and they are found in nice agreement especially with that of Kuznetsov and Nield [30].

The velocity, temperature , solutal concentration and nanoparticle fraction as well as the skin friction drag, wall heat transfer, regular mass transfer and nanoparticle mass transfer rates for some prescribed values of the various parameters $Pr,\ Nb,\ Nt, Nc,\ Nd, Nr,\ R, \gamma, M, Le, Ld, Ln, a$ and b are presented, briefly explained and illustrated graphically and in table form.

Figure - 1

Figure - 2
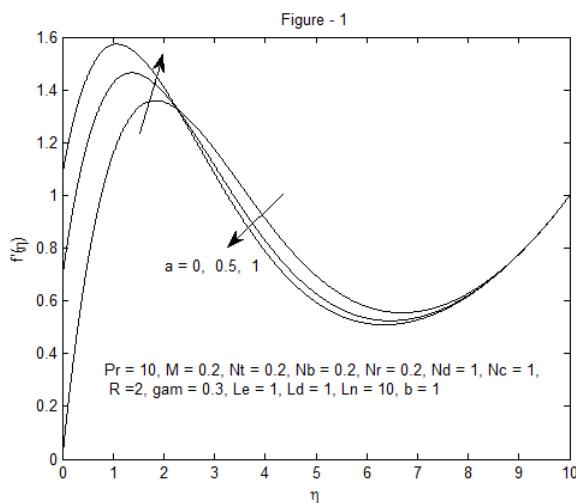
Fig.2(a): Effects of a on velocity profile
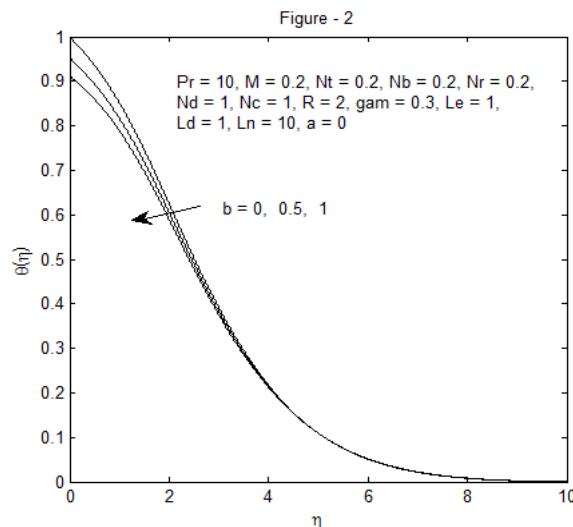
Fig.2(b): Effects of b on temperature profile

Fig.2(a) illustrates the effect of hydrodynamic slip parameter a on the velocity profile. It is verified that momentum slip condition assists the fluid to flow faster near the boundary layer. In this region, the fluid velocity gets the minimum for the no slip condition case ($a = 0$).The opposite may be true when we go farther and eventually, the graph decays to a single point as $\eta \to \infty$. Fig.2(b) shows the effect of thermal slip parameter to the temperature profile. It is observed that the temperature profile for the isothermal plate ($b = 0$) case gets the maximum than the non-isothermal plate ($b \neq 0$) case. It is apparent that thermal slip effect reduces the thermal boundary layer thickness because as the effect increases, more fluid will be transferred to the thermal boundary layer. Hence, rate of heat transfer will increase and as a result of this the thermal boundary layer decreases.

Figure - 3

Figure - 4
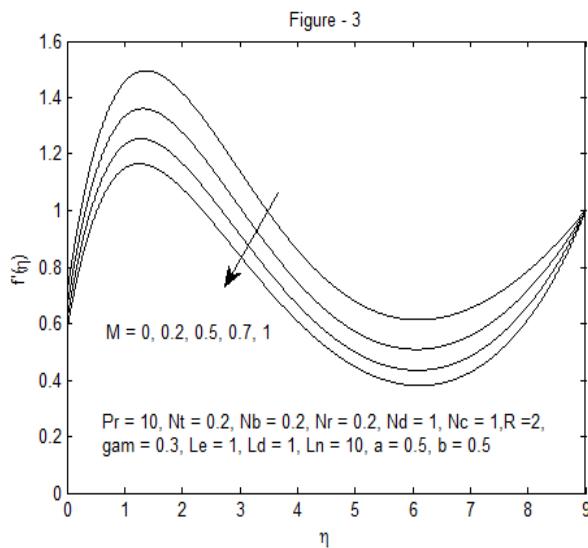
Fig.3: Effect of M on velocity profile
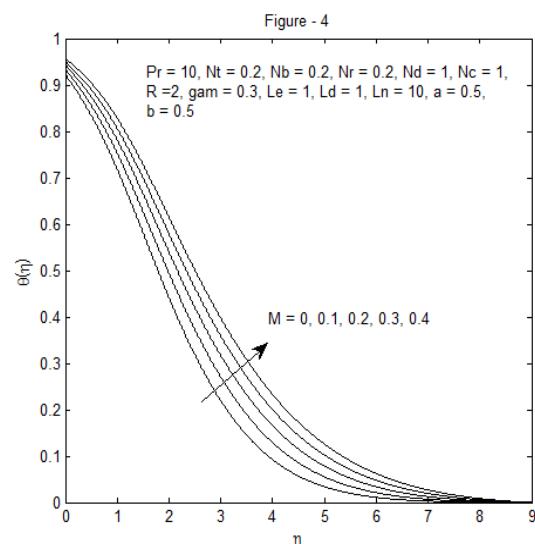
Fig.4: Effect of M on temperature profile

Fig.3 and Fig.4 show effects of magnetic parameter on velocity and temperature profiles, respectively. As it is expected, the presence of magnetic field retards the fluid velocity whereas it increases thermal boundary layer thickness. This occurs because as the intensity of the applied magnetic field increases in an electrically conducting fluid, it starts to produce the resistive Lorentz force. The force slows down the motion of the fluid in the boundary layer. The additional work done required to drag the nanofluid against the action of the magnetic field B is called thermal energy. This heats up the conducting nanofluid and upgrades the temperature profile. Thus, the presence of magnetic field in the flow regime decreases the momentum boundary layer thickness and enhances the thermal boundary layer thickness [33].
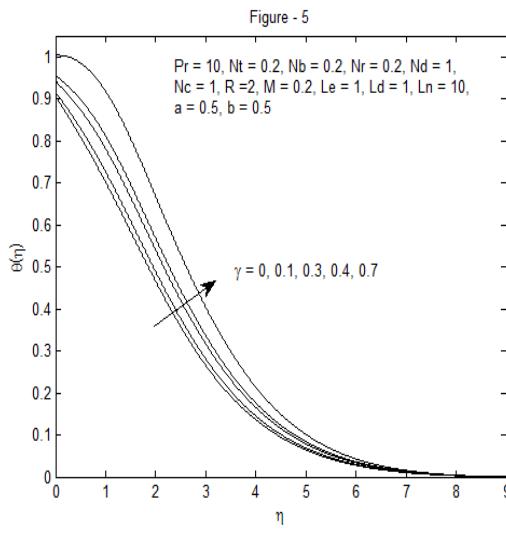
Fig.5: *Effect of* γ *on temperature profile*
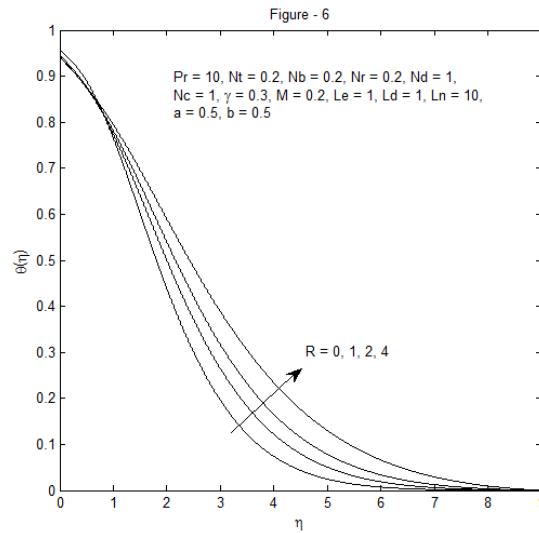

Fig.6: *Effect of* R *on temperature profile*

Fig.5 and Fig.6 illustrate the contributions of heat source/sink and thermal radiation effects on dimensionless temperature. It is observed that both parameters enhance the temperature profile. Thermal radiation is responsible in thickening the thermal boundary layer at the expense of releasing heat energy from the flow region and it causes the system to cool. In reality this is true because temperature increases as a result of increasing the Rosseland diffusion approximation for radiation q_r. Moreover, a rise in the values of heat source parameter γ increases both the velocity and temperature profiles. This is because the presence of source of heat in the flow enhances thermal energy and consequently, temperature will rise. The rise in temperature favours the fluid to increase the velocity profile due to the effect of buoyancy; the opposite is true for heat sink.
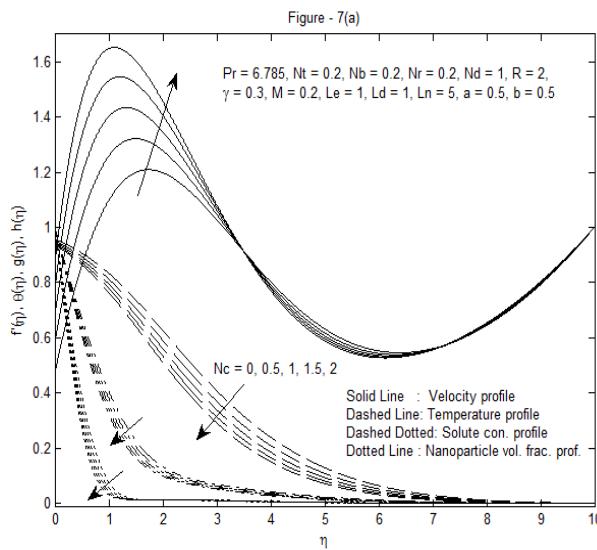
Fig.7(a): *Effects of* Nc *on vel., temp., solute con. and nanoparticle frac.prof.*
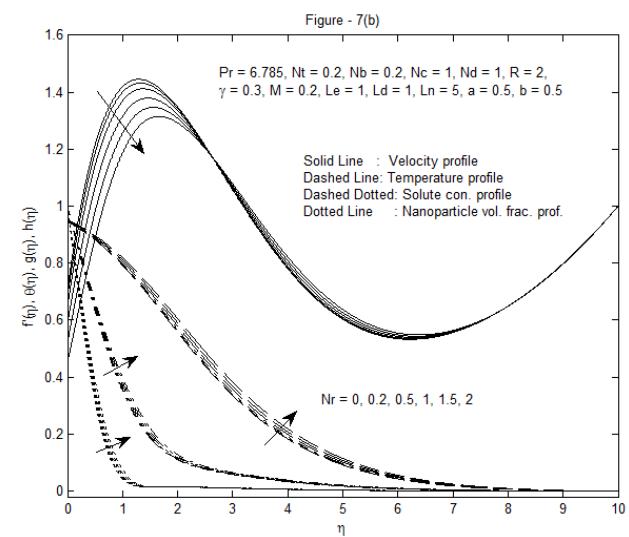
Fig.7(b): *Effects of* Nr *on vel., temp. solute conc. and nanoparticle fra. profiles*

Fig.7(a) and Fig.7(b) depict effects of regular buoyancy ratio parameter Nc and nanofluid buoyancy ratio parameter Nr on velocity, temperature, solutal concentration and nanoparticle volume fraction profiles. Increment of values of Nc assists the thickening of the momentum boundary layer but its change is not significant far away from the boundary layer. This is due to the fact that the buoyancy force acts like pressure gradient which accelerates/decelerates the fluid within the boundary layer [31]. But it reduces the temperature, solute concentration

and nanoparticle volume fraction profiles. On the other hand, roles of nanofluid buoyancy ratio parameter Nr play exactly the opposite of that of regular buoyancy ratio parameter $Nc.$
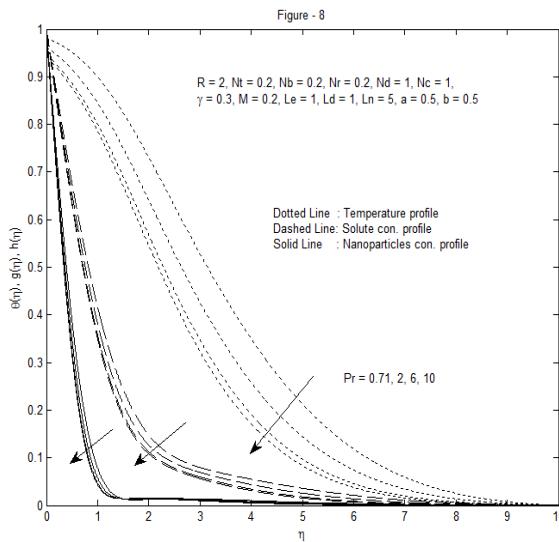

Fig.8: *Effects of Pr on velocity, solute concentration and nanoparticle fraction profiles*

Fig.8 exhibits the influence of Prandtl number on temperature, solute concentration and nanoparticle volume fraction profiles. The figure depicts that the higher the Prandtl number, the reduction will be the thermal, solute and nanoparticle boundary layer thickness. Prandtl number is a dimensionless number which is defined as the ratio of momentum diffusivity to thermal diffusivity, that is $Pr = \frac{\mu C_p}{k}$. Increasing the values of Pr implies that momentum diffusivity dominates thermal diffusivity. This means that thermal boundary layer thickness reduces at the expense of increasing the velocity profile with increasing values of Pr. Moreover, the nanoparticle volume fraction boundary layer thickness decreases but it exhibits overruns near the sheet for higher values of Pr.

Table 2: Effects of modified Dufour param. Nd and Prandtl number Pr on regular mass transfer rate $-g'(0)$.

Table -2

$-g'(0)$ for

$Nb = 0.2, Nt = 0.2, \ Nr = 0.2, \ Nc = 1, \ Ln = 10, \ Ld = 1, \ Le = 1, \ M = 0.2, \ \gamma = 0.3,$
$R = 2, \ a = 0.5, \ b = 0.5$

| Nd	$Pr = 0.71$	$Pr = 2$	$Pr = 6$	$Pr = 10$	$Pr = 50$
0	0.598124	0.638136	0.668011	0.677038	0.690849
1	0.676222	0.727140	0.764745	0.776158	0.793871
1.5	0.702967	0.758662	0.799872	0.812437	0.832059
2	0.724660	0.784703	0.829292	0.842959	0.864426
3	0.757707	0.825309	0.875998	0.891705	0.916647
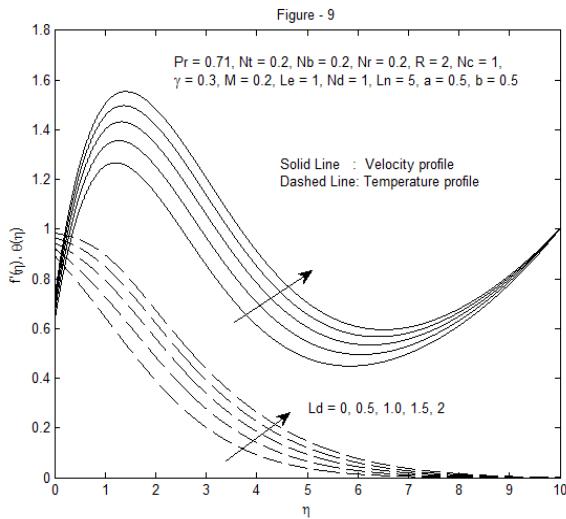
**Fig.9:** *Effects of Dufour solutal Lewis number Ld on velocity and temp. profiles*
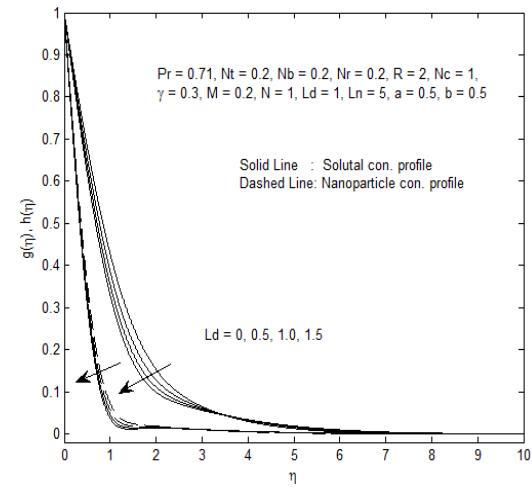
Fig.10: *Effects of Dufour solutal Lewis number Ld on solute conc. and nanopar.vol. fra. Profiles*

Fig.9 and Fig.10 show the effect of Dufour solutal Lewis number Ld on velocity, temperature, solute concentration and nanoparticle volume fraction profiles. This parameter enhances the thickening of both momentum and thermal boundary layers while it reduces that of solute and nanoparticle volume fraction.

Fig.11 and Fig.12 portray effects of Modified Dufour parameter Nd on velocity, temperature, solute concentration and nanoparticle volume fraction profiles. This parameter increases both momentum and thermal boundary layer thickness while it reduces that of solute and nanoparticle volume fraction
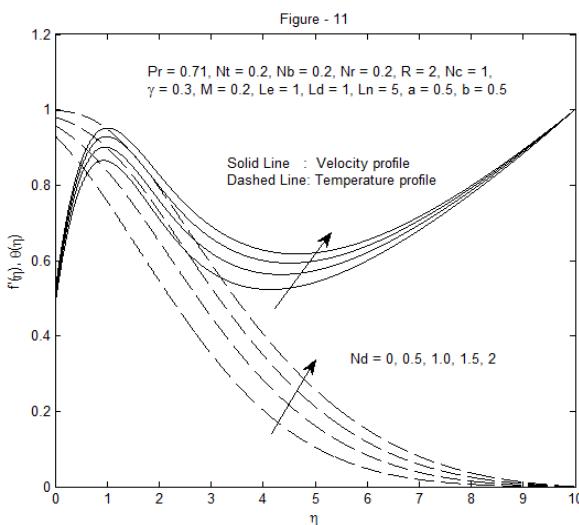
Fig.11: *Effect of modified Dufour parameter Nd on velocity and temperature profiles*
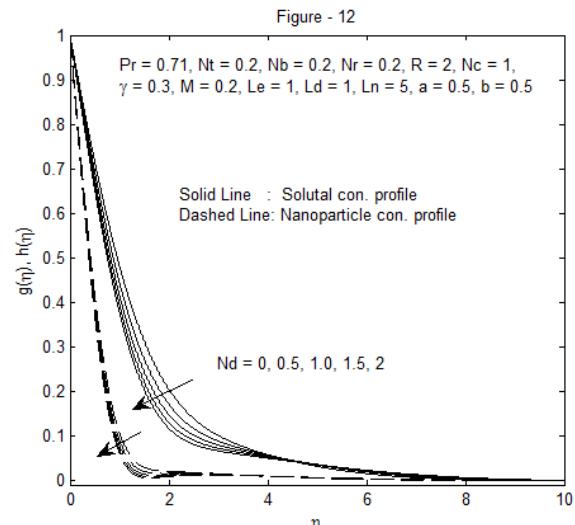
Fig.12: *Effect of modified Dufour parameter Nd on temp. and nanopar. vol. fra. profiles*

Effects of regular Lewis number Le on velocity, temperature and solute concentration profiles are shown in Fig.13. It is clearly shown that this parameter reduces both velocity and solute concentration profiles whereas it enhances the temperature profile. By definition, regular Lewis number is a dimensionless number which is the ratio of thermal diffusivity to mass diffusivity. Increasing the value of Le is the same as maximizing thermal boundary layer thickness at the expense of minimizing solutal boundary layer thickness which increases mass transfer rate.
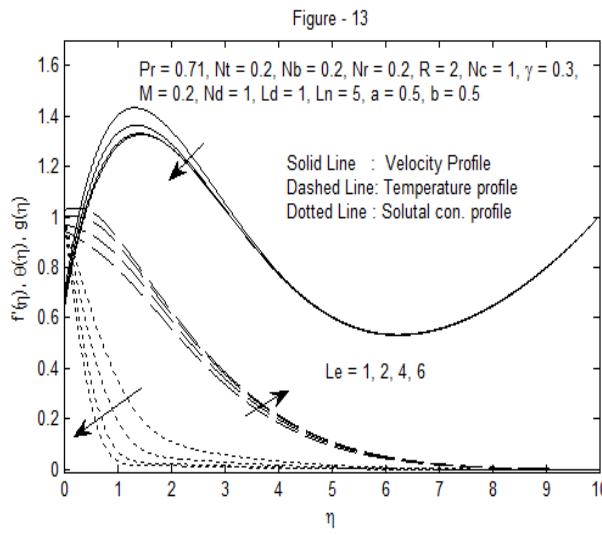
*Fig.13: Effects of regular Lewis number Le on velocity, temp. and solute conc. profiles*
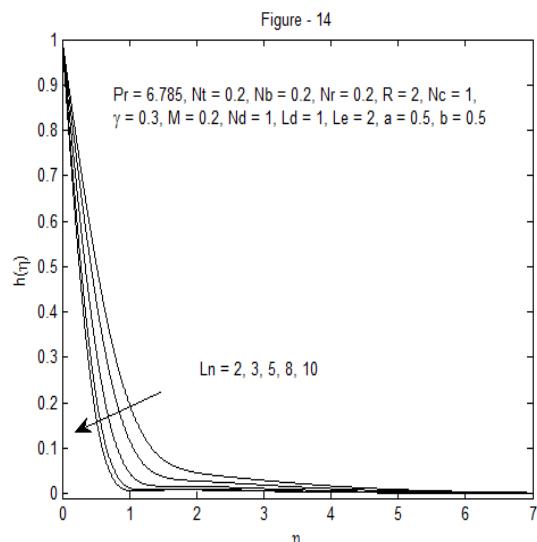
Fig.14: The effect of nanofluid Lewis number Ln on nanoparticle fraction profile

Fig.14 illustrates the effect of nanofluid Lewis number Ln on nanoparticle volume fraction profile. It is clearly shown that as the value of the parameter Ln increases, nanoparticle volume fraction boundary layer thickness decreases. By definition, Ln is the ratio of thermal diffusivity α to Brownian motion diffusion coefficient D_B. Increasing the value of Ln implies that D_B is decreasing and hence, the nanoparticle volume fraction boundary layer thickness decreases.

Table 3: Effects of modified Dufour parameter Nd and Prandtl number Pr on nanoparticle mass transfer rate $-h'(0)$.

Table – 3

$-h'(0)$ for

$Nb = 0.2, Nt = 0.2,\ Nr = 0.2,\ Nc = 1,\ Ln = 10,\ Ld = 1,\ Le = 1,\ M = 0.2,\ \gamma = 0.3,$
$R = 2,\ a = 0.5,\ b = 0.5$

Nd	$Pr = 0.71$	$Pr = 2$	$Pr = 6$	$Pr = 10$	$Pr = 50$
0	1.782304	1.915290	2.004483	2.029976	2.067935
1	1.848910	2.001989	2.108922	2.140340	2.188160
1.5	1.871990	2.033157	2.147552	2.181561	2.233806
2	1.890788	2.059083	2.180220	2.216621	2.273013
3	1.919523	2.099814	2.232701	2.273387	2.3373720

Fig.15 and Fig. 16 show effects of magnetic field and heat source on skin friction coefficient, rate of heat transfer, regular mass transfer and nanoparticle mass transfer rates. It is observed that M decreases all quantities $f''(0)$,

$-\theta'(0)$, $-g'(0)$ and $-h'(0)$. This is true because, as M gets larger there is a tendency to increase thermal, solute and nanoparticle boundary layer thickness and consequently, it decreases the rate of heat transfer, regular mass transfer and nanoparticle mass transfer rates. On the other hand, heat source reduces the rate of heat transfer while it enhances both regular mass transfer and nanoparticle mass transfer rates.

Fig.17 exhibits the effect of thermal radiation on skin friction coefficient. As R increases skin friction coefficient increases rapidly. Influences of nanofluid buoyancy ratio parameter Nr and regular buoyancy ratio parameter Nc on skin friction coefficient are illustrated in Fig.18. The figure indicates that $f''(0)$ is an increasing function of Nc but it decreases with Nr.
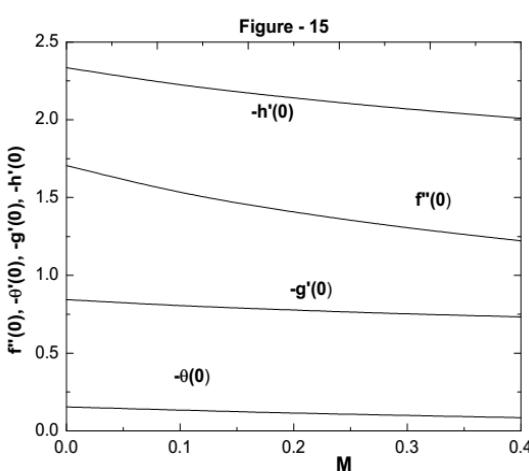
**Fig.15: Effects of magnetic parameter M on $-\theta'(0)$, $-g'(0)$ and $-h'(0)$**
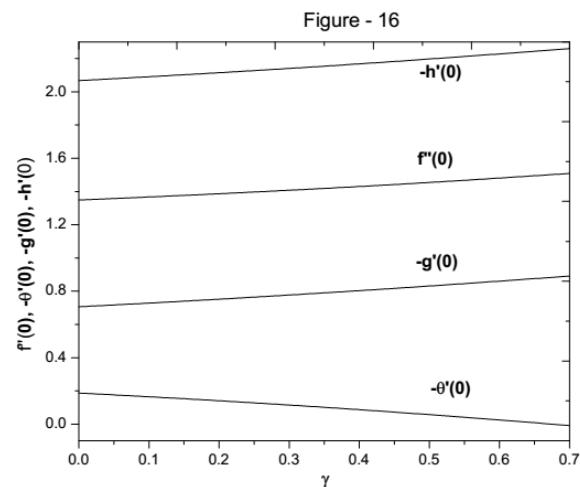
Fig.16: Effects of heat source/sink parameter γ $f''(0)$, on $f''(0)$, $-\theta'(0)$, $-g'(0)$ and $-h'(0)$
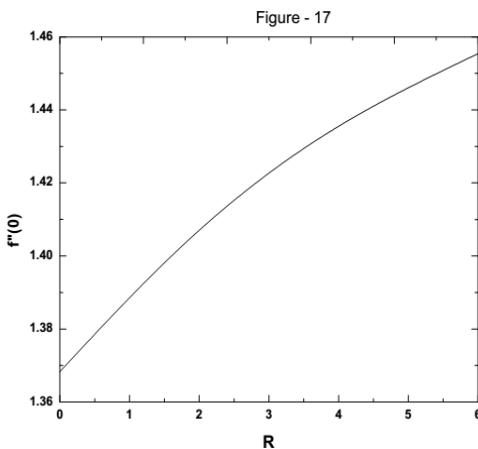

**Fig.17: The effect of radiation parameter R on friction coefficient $f''(0)$**
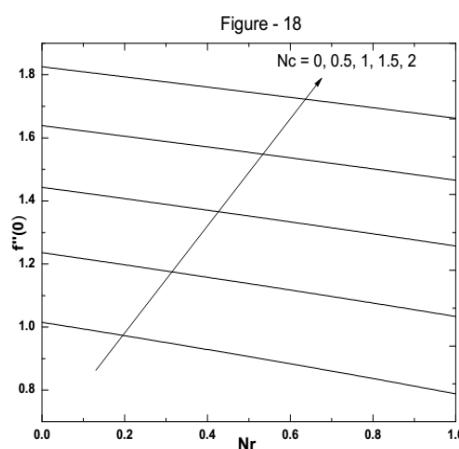
**Fig.18: Effects of Nr and Nc on skin friction skin coefficient $f''(0)$**
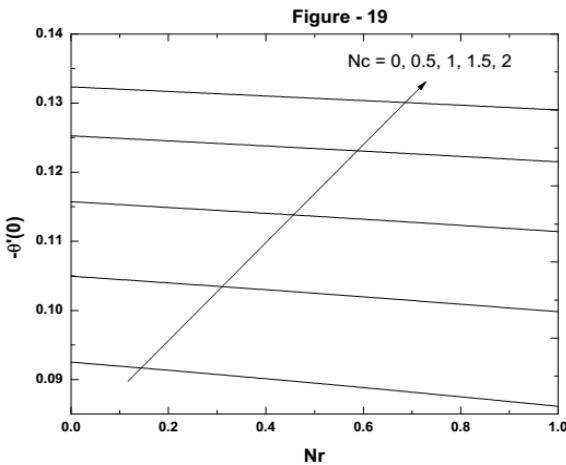
Fig.19: *Effects of Nanofluid buoyancy ratio Nr and Regular buoyancy ratio Nc parameters on heat transfer rate $-\theta'(0)$*
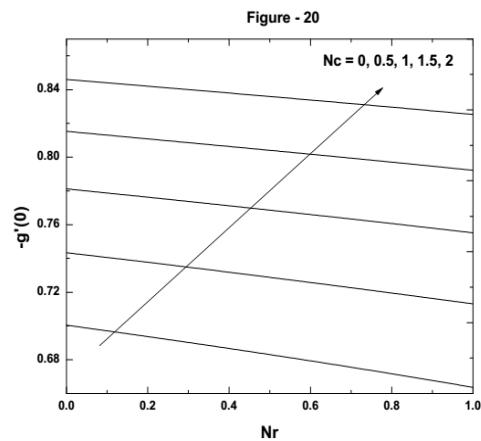
Fig.20: *Effects of Nanofluid buoyancy ratio Nr and Regular buoyancy ratio Nc parameters on regular mass transfer rate $-g'(0)$*

Table 2, Table 3, Fig.22 and Fig.23 describe the roles of modified Dufour parameter Nd and Prandtl number Pr on regular mass transfer rate, nanoparticle mass transfer rate, skin friction coefficient and heat transfer rate, respectively. It is observed that both Nd and Pr increase the values of regular mass transfer rate, nanoparticle mass transfer rate and skin friction coefficient. On the other hand, $-\theta'(0)$ is an increasing function of Pr but it decreases with increasing values of Nd. This is due to the fact that the higher the Prandtl number the thinner the thermal, solutal and nanoparticle volume fraction boundary layers (refer Fig.8). As a result of this, the rate of heat and mass diffusion increase with increasing values of Pr. Moreover, Nd contributes to the thickening of thermal boundary layer (refer Fig.11) and thinning the solute concentration and nanoparticle volume fraction boundary layers (refer Fig.12). This in turn results in lowering the heat transfer rate and raising both regular mass transfer and nanoparticle mass transfer rates.
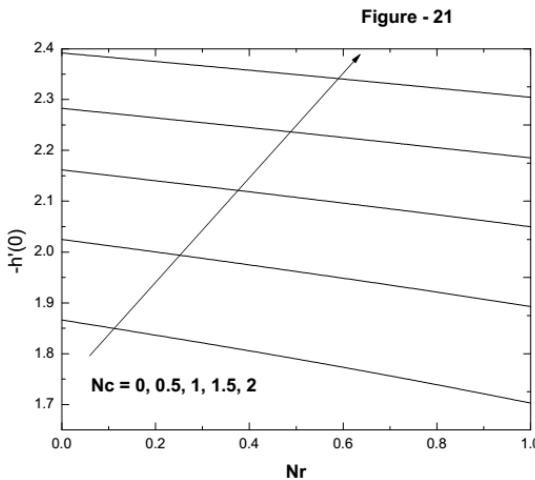

Fig.21: *Effects of Nanofluid buoyancy ratio Nr and Regular buoyancy ratio Nc parameters on nanoparticle mass transfer rate $-h(0)$*
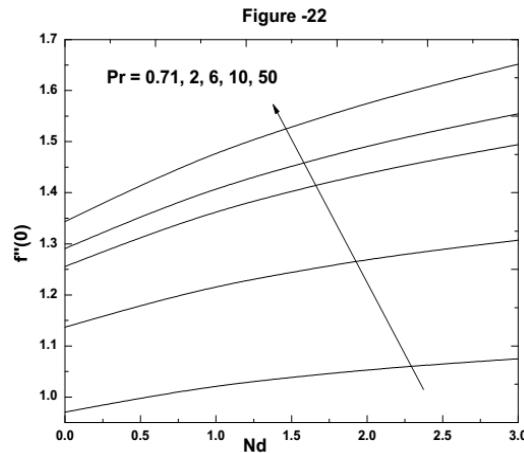
Fig.22: *Effects of Prandtl number Pr and modified Dufour parameter Nd on skin friction coeff. $f''(0)$*

Fig.19-Fig.21 describe roles of nanofluid buoyancy ratio parameter Nr and regular buoyancy ratio parameter Nc on heat transfer, regular mass transfer and nanoparticle mass transfer rates. The figures indicate that the heat and mass transfer rates are increasing functions of Nc but all decrease with increasing values of Nr. This is due to the fact that the higher the regular buoyancy ratio parameter Nc the thinner the thermal, solutal and nanoparticle volume fraction boundary layers (refer Fig.7(a)). As a result of this, heat and mass diffusion rates increase with increasing values of Nc. The roles of Nr play exactly the opposite to that of Nc (refer Fig.7(b)) and so does for rates of heat and mass transfers.
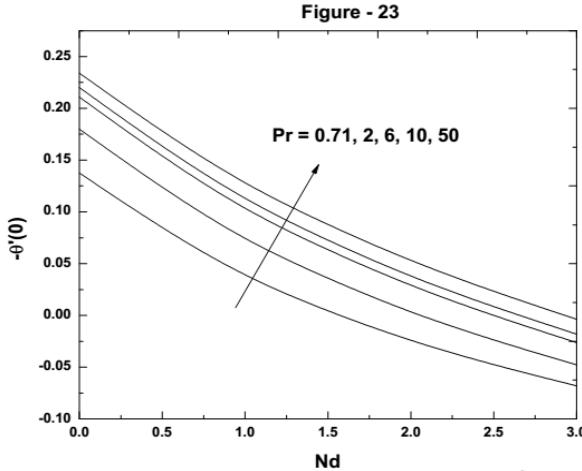

Fig.23: Effects Pr and Nd on heat tran. rate $-\theta'(0)$.
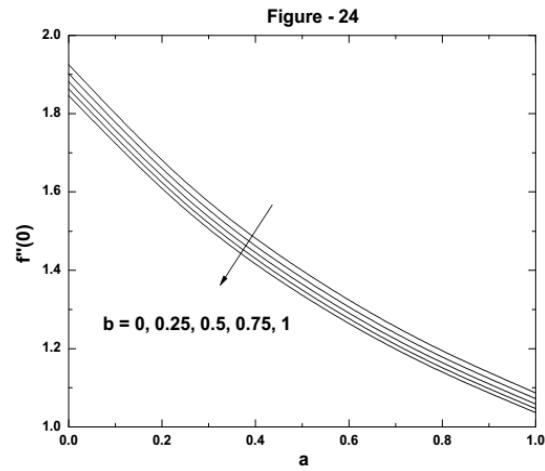

Fig.24: Effects of a on skin fric. coeff. $f''(0)$.

Fig.24-Fig.26 and Table 4 show influences of hydrodynamic slip parameter a and thermal slip parameter b on skin friction coefficient, wall heat transfer rate, regular mass transfer rate and nanoparticle mass transfer rate, respectively. The presence of thermal slip condition reduces skin friction coefficient, heat and mass transfer rates. On the other hand, hydrodynamic slip condition reduces skin friction coefficient but it enhances all heat and mass transfer rates.
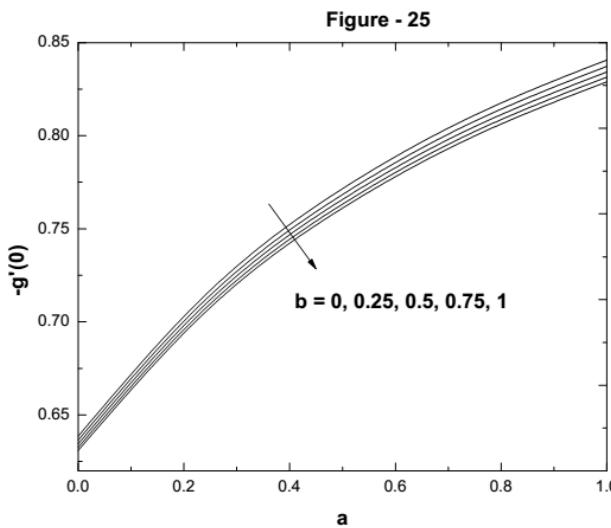

Fig.25: Effects of a and b on $-g'(0)$.
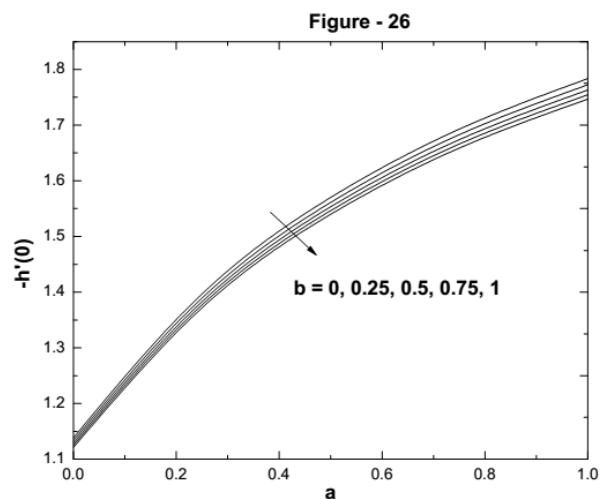

Fig.26: Effects of a and b on $-h'(0)$.

Fig.27, Fig.28 and Table5 show how much the parameters Dufour solutal Lewis number Ld and nanofluid Lewis number Ln on skin friction coefficient, regular and nanoparticle mass transfer rates, respectively. As the parameter Ld increases, skin friction coefficient, heat transfer rate and regular mass transfer rate increase while it reduces

nanoparticle mass transfer rate. On the other hand, Ln enhances skin friction coefficient, heat and mass transfer rates.

Table 4: Effects of momentum and thermal slip parameters on the rate of heat transfer $-\theta'(0)$

Table – 4				
$\theta'(0)$ for				
Pr = 6.785, Nb = 0.2, Nt = 0.2, Nr = 0.2, Nc = 1, Nd = 1, Le = 1, Ln = 5, Ld = 1, M = 0.2, γ = 0.3, R = 2				
a	$b = 0$	$b = 0.25$	$b = 0.5$	$b = 0.75$	$b = 1$
0	0.102086	0.096232	0.091054	0.086438	0.082292
0.25	0.112822	0.105664	0.099415	0.093906	0.089008
0.5	0.120897	0.112712	0.105631	0.099436	0.093965
0.75	0.127078	0.118082	0.110350	0.103623	0.097711
1	0.131914	0.122269	0.114020	0.106873	0.100613
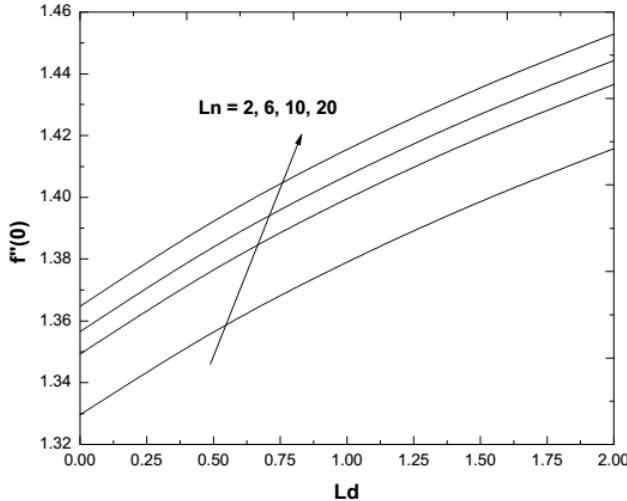
*Fig.27: Effects of Ln and Ld on skin fric. Coeff. $f''(0)$.* *Fig.28: Effects of Ln and Ld on $-g'(0)$*
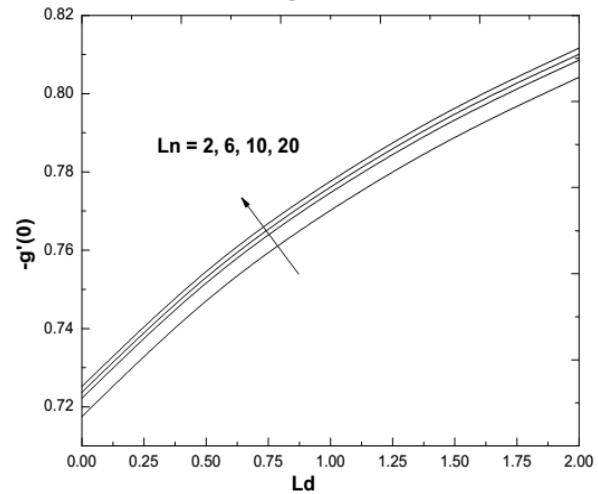
As effects of Brownian motion parameter Nb and thermophoresis parameter Nt on skin friction coefficient, heat transfer rate, regular mass transfer rate and nanoparticle mass transfer rate are briefly explained [2] and this is in conformity to our study, we didn't incorporate their effects in the paper.

Table 5: Effects of Nanofluid Lewis number Ln and Dufour solutal Lewis number Ld on nanoparticle mass transfer rate $-h'(0)$.

Table -5

$h'(0)$ for

$Pr = 10, Nb = 0.2, Nt = 0.2, Nr = 0.2, Nc = 1, Nd = 1, Le = 1, M = 0.2, \gamma = 0.3,$
$R = 2, a = 0.5, b = 0.5$

Ld	$Ln = 0$	$Ln = 2$	$Ln = 6$	$Ln = 10$	$Ln = 20$
0	0.125842	1.036811	1.683197	2.113061	2.890357
0.5	0.117001	1.041731	1.693674	2.127792	2.912988
1	0.111271	1.046081	1.702688	2.140340	2.932095
1.5	0.107335	1.049985	1.710582	2.151237	2.948560
2	0.104531	1.053516	1.717577	2.160822	2.962953

5. Conclusions

Momentum and thermal slip conditions of an MHD double diffusive free convective boundary layer flow of a nanofluid with radiation and heat source/sink effects past a vertical semi-infinite flat plate situated in a free stream have been studied. The governing equations associated to the boundary conditions were transformed into a system of ODEs with the help of similarity transformation equations. Solutions of these problems are solved numerically with the help of the shooting technique along with the fourth order Runge-Kutta integration scheme. Some of the results obtained from the study among others are the following:

- The velocity profile in the boundary layer decreases with an increase in the values of regular Lewis number, magnetic parameter and nanofluid buoyancy ratio parameter whereas it increases with an increase in the values of momentum slip parameter, regular buoyancy ratio number, modified Dufour parameter and Dufour solutal Lewis number.
- Dufour solutal Lewis number, heat source parameter, radiation parameter, regular Lewis number, nanofluid buoyancy ratio parameter, magnetic parameter and modified Dufour parameter enhance the temperature profile whereas regular buoyancy ratio parameter, thermal slip parameter and Prandtl number reduce the temperature profile.
- Solutal concentration profile is enhanced by nanofluid buoyancy ratio parameter whereas regular Lewis number, Prandtl number, regular buoyancy ratio number, modified Dufour parameter and Dufour solutal Lewis number reduce the solutal concentration profile.
- Nanoparticle volume fraction profile is enhanced by nanofluid buoyancy ratio parameter whereas nanofluid Lewis number, Prandtl number, regular buoyancy ratio number, modified Dufour parameter and Dufour solutal Lewis number reduce the nanoparticle volume fraction profile.
- Increasing the values of the nanofluid Lewis number, radiation parameter, regular buoyancy ratio parameter, Prandtl number, modified Dufour parameter, Dufour solutal Lewis number and source of heat parameter enhance the skin friction coefficient whereas it decreases with increasing values of thermal slip, momentum slip, nanofluid buoyancy ratio and magnetic parameters.

- The presence of Prandtl number, momentum slip and regular buoyancy ratio parameters in the flow field is to enhance the rate of heat transfer whereas magnetic, nanoparticle buoyancy ratio, modified Dufour, thermal slip and source of heat parameter are to minimize it.

- Increasing the values of the nanofluid Lewis number, momentum slip parameter, regular buoyancy ratio parameter, Prandtl number, modified Dufour parameter, Dufour solutal Lewis number and source of heat parameter enhance the regular mass transfer rate whereas it decreases with increasing values of thermal slip, nanofluid buoyancy ratio and magnetic parameters.

- Nanoparticle mass transfer rate is an increasing function of momentum slip parameter, regular buoyancy ratio parameter, source of heat parameter, modified Dufour parameter and Prandtl number whereas it decreases with increasing values of Dufour solutal Lewis number, thermal slip, nanofluid buoyancy ratio and magnetic parameters.

References

[1] Kaufui, V, Wong & Omar, De, Leon. (2010). Applications of nanofluids: current and future. Advances in Mech. Eng.; ID 519659, doi:10.1155/2010/519659.

[2] SlifGupta, HK, Agrawal, GD & Mathur, J. (2012). An overview of Nanofluids: A new media towards green environment. Int. of Envi. Sci.; 3(1): 433-440.

[3] Xiang, QW & Arun, SM. (2008). A review on nanofluids-experiments and applications. Brazilian J. of Chem. Eng.; 25(4): 631–648.

[4] Choi, SU & Eastman, JA. (1995). Enhancing thermal conductivity of fluids with nanoparticles. Developments and App of Non-Newtonian Flows FED; 66: 99–105.

[5] Buongiorno, J. (2006). Convective transport in nanofluids. ASME J. Heat Trans.; 128: 240-250.

[6] Crane, LJ. (1970). Flow past a stretching plate. J Appl. Math. Phys. (ZAMP); 21: 645–647.

[7] Khana, WA & Aziz, A. (2011). Natural convection flow of a nanofluid over a vertical plate with uniform surface heat flux. Int. J. of Thermal Sciences; 50: 1207-1214.

[8] Kuznetsov, AV & Nield, DA. (2010). Natural convective boundary layer flow of a nanofluid past a vertical plate. Int. J. Thermal Sci.; 49: 243–247.

[9] Aziz, A & Khan, WA. (2012). Natural convective boundary layer flow of a nanofluid past a convectively heated vertical plate. Int. J. of Thermal Sciences; 52: 83-90.

[10] Khan, WA & Pop, I. (2010). Boundary-layer flow of a nanofluid past a stretching sheet. Int. J. Heat Mass Tran.; 53: 2477–2483.

[11] Makinde, OD. (2005). Free-convection flow with thermal radiation and mass transfer past a moving vertical porous plate. Int. Comm. Heat and Mass Trans.; 32 (10): 1411–1419.

[12] Cheng, P & Minkowycz, WJ. (1977). Free convection about a vertical flat plate embedded in a porous medium with application to heat transfer from a dike. J Geophysics Research; 82 (14): 2040–2044.

[13] Rahman, MM & Eltayeb, IA. (2013). Radiative heat transfer in a hydromagnetic nanofluid past a nonlinear stretching surface with convective boundary condition. Mecc.; 48: 601–615.

[14] Nield, DA & Kuznetsov, AV. (2011). The Cheng–Minkowycz problem for the double-diffusive natural convective boundary-layer flow in a porous medium saturated by a nanofluid. Int. J. Heat Mass Trans.; 54: 374–378.

[15] Reddy, G. (2014). Influence of thermal radiation, viscous dissipation and hall current on MHD convection flow over a stretched vertical flat plate. Ain Shams Engineering Journal; 5: 169-175.

[16] Khan, MS, Karim, I, Ali, LE & Islam, A. (2012). Unsteady MHD free convection boundary-layer flow of a nanofluid along a stretching sheet with thermal radiation and viscous dissipation effects. Int. Nano Lett.; doi:10.1186/2228-5326-2-24.

[17] Khana, WA & Aziz, A. (2011). Double-diffusive natural convective boundary layer flow in a porous medium saturated with a nanofluid over a vertical plate: Prescribed surface heat, solute and nanoparticle fluxes. Int. J. of Thermal Sciences; 50: 2154-2160.

[18] Capretto, L, Cheng, W, Hill, M & Zhang, X. (2011). Micromixing within microfluidic devices. Top Curr. Chem.; 304: 27–68.

[19] Kleinstreuer, C, Li, J & Koo, J. (2008). Microfluidics of nano-drug delivery. Int J Heat Mass Transfer; 51: 5590–5597.

[20] Yazdi, MH, Abdullah, S, Hashim, I & Sopian, K. (2011). Slip MHD liquid flow and heat transfer over non linear permeable stretching surface with chemical reaction. Int. J. Heat Mass Transfer; 54: 3214–3225.

[21] Uddin, MJ, Khan ,WA & Ismail, AI. (2012). MHD free convective boundary layer flow of a nanofluid past a flat vertical plate with Newtonian heating boundary condition. PLoS ONE; 7(11): doi:10.1371/journal.pone.0049499.

[22] Chamkha, AJ & Aly, AM. (2011). MHD free convection flow of a nanofluid past a vertical plate in the presence of heat generation or absorption effects. Chem. Eng. Comm.; 198: 425–441.

[23] Srinivasacharya, D & Surender, O. (2014). Non-similar solution for natural convective boundary layer flow of a nanofluid past a vertical plate embedded in a doubly stratified porous medium. Int. J. of Heat and Mass Transfer; 71: 431–438.

[24] Olanrewaju, PO, Alao, FI, Adeniyan, A & Bishop SA. (2013). Double diffusive convection from a permeable vertical surface under convective boundary condition in the presence of heat generation and thermal radiation. Nonlinear Sci. Lett. A; 4(3): 76-90.

[25] Swati, M. (2013). Slip effects on MHD boundary layer flow over an exponentially stretching sheet with suction/blowing and thermal radiation. Ain Shams Engineering J.; 4: 485-491.

[26] B´eg, OA, Uddin, MJ, Rashidi, MM & Kavyani, N. (2015). Double diffusive radiative magnetic mixed convective slip flow with Biot and Richardson number effects. J. of Engineering Thermophysics; 23 (2): 79–97.

[27] Aziz, A. (2009). A similarity solution for laminar thermal boundary layer over a flat plate with a convective surface boundary condition. Comm. Nonlin. Sci. Numer. Simul.; 14: 1064–1068.

[28] Nandeppanavar, MM, Vajravelu, K, Abel, MS & Siddalingappa, MN. (2012). Second order slip flow and heat transfer over a stretching sheet with non-linear Navier Boundary Condition. *Int. J. Therm. Sci.*b; 58: 143–150.

[29] Khan, WA, Uddin, Md J & Ismail, AI Md. (2013). Hydrodynamic and thermal slip effect on double diffusive free convective boundary layer flow of a nanofluid past a flat vertical plate in the moving free stream. PLoS ONE; 8(3): doi:10.1371/journal.pone.0054024.

[30] Kuznetsov, AV & Nield, DA. (2011). Double-diffusive natural convective boundary layer flow of a nanofluid past a vertical surface. Int J Therm Sci.; 50: 712–717.

[31] RamReddy, Ch, Murthy, SN, Chamkha, AJ &Rashad, AM. (2013). Soret effect on mixed convection flow in a nanofluid under convective boundary condition. Int. J. of Heat and Mass Transfer; 64: 384–392.

[32] Mandal, C & Mukhopadhyay, S. (2013). Heat transfer analysis for fluid flow over an exponentially stretching porous sheet with surface heat flux in porous medium. *Ain Shams Eng. J.;* 4 (1): 103-110.

[33] Goyal, M & Bhargava, R. (2013). Numerical solution of MHD viscoelastic nanofluid flow over a stretching sheet with partial slip and heat source/sink. ISR N Nano technology; 2013: ID. 931021, http://dx.doi.org./10.1155/2013/931021.